

# MEASUREMENTS OF ANTIDEUTERON ABSORPTION AND STRIPPING CROSS SECTIONS AT THE MOMENTUM 13.3 GeV/c

S. P. DENISOV, S. V. DONSKOV, Yu. P. GORIN, V. A. KACHANOV,  
V. M. KUTJIN, A. I. PETRUKHIN, Yu. D. PROKOSHKIN,  
E. A. RAZUVAEV, R. S. SHUVALOV and D. A. STOJANOVA  
*Institute for High Energy Physics, Serpukhov, USSR*

Received 11 December 1970

**Abstract:** The absorption cross sections of antideuteron with the momentum  $P = 13.3$  GeV/c by Li, C, Al, Cu and Pb nuclei have been measured. Antiproton stripping of antideuteron has been registered and its cross section for C, Al and Cu has been defined. The binding energy of antideuteron is found to be  $\epsilon_{\bar{d}} = 2.4 \pm 0.6$  MeV by measuring the angular distribution of antiprotons from stripping.

## 1. INTRODUCTION

The launching of the 70 GeV accelerator has opened up the possibilities for carrying out quantitative investigations of high-energy antideuteron interactions with matter. The antideuteron beam intensity at this accelerator amounts to several tens of thousands of antideuteron per day [1] that is two orders of the magnitude higher than at the accelerators of lower energy [2].

The first measurements of the cross sections for antideuteron interaction with nuclei were made at the momentum 25 GeV/c [3]. The directly measured values in the experiment were the cross sections  $\sigma'_a = \sigma_a - \sigma_{\bar{p}\text{str}}$ ; that is, the cross sections of all the inelastic processes  $\sigma_a$  excluding the cross sections  $\sigma_{\bar{p}\text{str}}$  of processes where antideuteron stripping with forward emission of one antiproton took place. In order to calculate the absorption cross section  $\sigma_a$ , corrections were introduced for the stripping process and they amounted to 40% for light nuclei. These corrections were obtained with from calculations where the Glauber multiple scattering model [4] and the Monte Carlo method [5] were used.

The present paper reports on the data on direct measurements of the cross sections of antideuteron absorption by Li, C, Al, Cu and Pb nuclei. Unlike the earlier work [3] the particles emitted from the investigated target, were analyzed by their momentum with a magnet. This allowed one to select the process where the antiproton is stripped off the antideuteron and to define its cross sections as well as the binding energy of antideuteron.

The measurements were made in the beam with the momentum ( $P =$

= 13.3 GeV/c) that corresponded to the maximum antideuteron yield at the energy of accelerated protons  $E_0 = 70$  GeV/c. The antideuteron flux was by one order of magnitude higher than in earlier experiments [3]. It allowed us to improve the measurement accuracy of the cross sections several fold.

## 2. EXPERIMENTAL APPARATUS

The negative secondary beam with momentum 13.3 GeV/c produced by accelerated protons on the internal Al target was ejected into the magnetic-optic beam channel [6] at an angle of 47 mrad. Fig. 1 presents the layout of the experimental apparatus along the beam channel. The particle beam was defined by scintillation counters  $S_1$ - $S_7$  switched in coincidence and by a guard counter A with a hole in the centre. The coincidence counting rate  $M = S_1 S_2 S_3 S_4 S_5 S_6 S_7 \bar{A}$  was  $\approx 8 \cdot 10^5$  per accelerator cycle at a momentum spread of  $\pm 2\%$  and a spill duration of the accelerated proton beam onto the internal target of  $\approx 0.7$  sec.

The gas Čerenkov counters with quartz optics were used to separate antideuterons from other beam particles, 90% of which were pions. The threshold counters  $C_1$  and  $C_2$  (refs. [7, 8]) 1.5 m long were switched in anticoincidence with the M signal and suppressed the counting of antiprotons and other light particles. The great amount of Čerenkov light produced by the particles in these counters (fig. 2) allowed us to suppress the counting of the particles lighter than antideuteron up to the level  $\lesssim 3 \cdot 10^{-9} M$ . The 1m long differential Čerenkov counter D (refs. [8, 9]) switched in coincidence was tuned for registering antideuterons (fig. 3). The counting rate of antideuterons striking the target defined by the signal  $V = M \bar{C}_1 \bar{C}_2 D$  was  $\approx 2$  per cycle. It corresponded to a relative antideuteron content in the beam  $V/M \approx 2.5 \cdot 10^{-6}$ . During the measurements, approximately  $2 \cdot 10^4$  antideuterons have been registered. The contamination of other particles with  $P = 13.3$  GeV/c amounted to  $\ll 10^{-3}$ .

The antideuteron beam that passed through the target and the particles produced in the target were momentum analysed with the help of the magnet  $M_5$ . Antiprotons from the antideuteron stripping in the counters situated in front of the target, were ejected from the beam by the magnet  $M_5$  and were not registered by the counters situated behind the magnet (the antiproton contamination in the antideuteron beam striking the target was  $\approx 0.5\%$ ).

The measurements of the absorption cross sections were carried out by

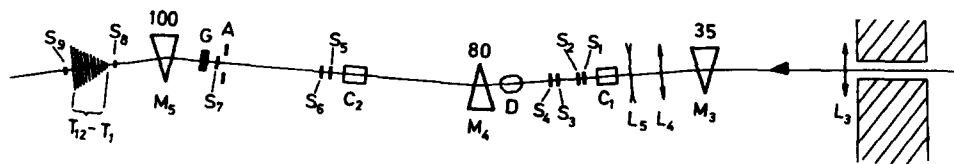


Fig. 1. The layout in the negative-particle beam (the beginning of the magnetic-optic beam channel [6] is not shown).  $M_3$ - $M_5$  are bending magnets, the figures indicate the angles of the beam deflection in mrad;  $L_3$ - $L_5$  are quadrupole lenses; G is a target;  $S_1$ - $S_9$  are scintillation counters;  $T_1$ - $T_{12}$  are transmission counters;  $C_1$ ,  $C_2$  are threshold Čerenkov counters; D is a differential Čerenkov counter.

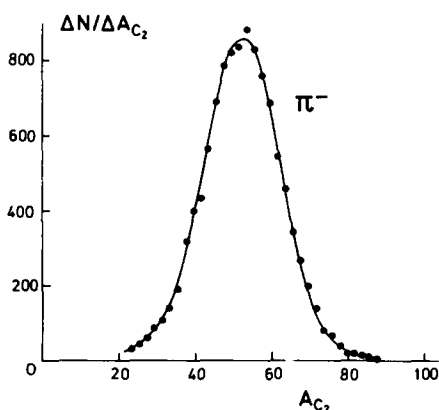


Fig. 2. Pulse-height spectrum for the threshold Čerenkov counter  $C_2$ . The width of the spectrum corresponds to the average number of the knocked out photoelectrons from the photomultiplier photocathode  $\approx 40$ .

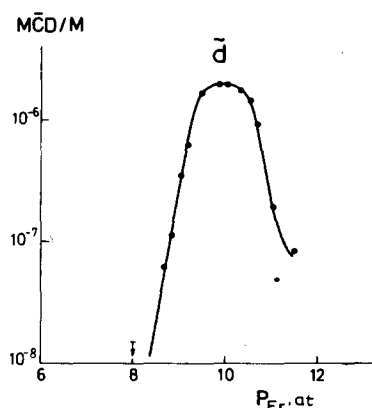


Fig. 3. The dependence of the antideuteron counting rate upon the pressure of freon in the differential Čerenkov counter D.

the transmission-counter technique described earlier [10]. Twelve transmission counters  $T_1$ - $T_{12}$  were situated behind the magnet  $M_5$  at a distance of  $\approx 8$  m from the target. They registered the scattered particles in the momentum-transfer-squared  $t$  interval  $0.007 \leq |t| \leq 0.112$  ( $\text{GeV}/c$ )<sup>2</sup>. In the course of measurements different targets were introduced into the beam in sequence; the counting rate of the V-signal coincidences with the signals from the transmission counters were registered together with accidental coincidences (they comprised  $< 1\%$ ) and the efficiency of each of the  $i$ th channels was  $> 99.5\%$ . Small counters  $S_8$ ,  $S_9$  with diameters 1 and 2 cm, correspondingly, were used for measuring the efficiency.

### 3. ABSORPTION CROSS SECTIONS

The data obtained in the interval  $0.054 \leq |t| \leq 0.112$  ( $\text{GeV}/c$ )<sup>2</sup>, where the contribution from elastic scattering of antideuterons may be neglected, were used for extrapolation of the partial cross sections  $\sigma_i$  measured by the counters  $T_i$  to the zero value of  $t$ . The dependence:

$$\sigma_i(t) = \sigma_a \exp(bt), \quad (1)$$

was used in the extrapolation. This dependence gives a good description of the measured partial cross sections for all the targets. The obtained absorption cross sections are given in table 1 and in fig. 4.

The absorption cross sections were also measured for negative pions, kaons and antiprotons with  $P = 13.3$   $\text{GeV}/c$  (fig. 4). These measurements were performed not only using the above mentioned technique, but also without the use of the magnet  $M_5$ . In the latter case the transmission counters

Table 1  
Absorption and stripping cross sections (mb) of antideuterons at  $P = 13.3$  GeV/c.

Target	Target thickness (g/cm <sup>2</sup> )	$\sigma_a$	$\sigma_{\bar{p}\text{str}}$	$\xi = \frac{\sigma_{\bar{p}\text{str}}}{\sigma_a}$	$\sigma_a^*$ (P = 25 GeV/c)
Li	20.7	390 ± 20			360 ± 40
C	40.6	535 ± 27	175 ± 20	0.34 ± 0.04	510 ± 85
Al	37.8	845 ± 43	235 ± 45	0.28 ± 0.66	835 ± 140
Cu	39.1	1300 ± 130	280 ± 70	0.23 ± 0.05	1480 ± 200
Pb	36.6	3000 ± 300			3700 ± 670

\* Cross sections at  $P = 25$  GeV/c calculated with the data [3] using corrections for antiproton stripping of antideuterons equal to 0.5 (see the text).

were installed along the beam continuation and they registered the secondaries with low momenta which were ejected from the beam when the magnet was in operation. The results on the absorption cross sections obtained by both techniques coincided within the measurement errors and are in good accord with the data obtained earlier [3, 10]. In all the cases the agreement between the measured partial cross sections and dependence [1] appeared to be satisfactory.

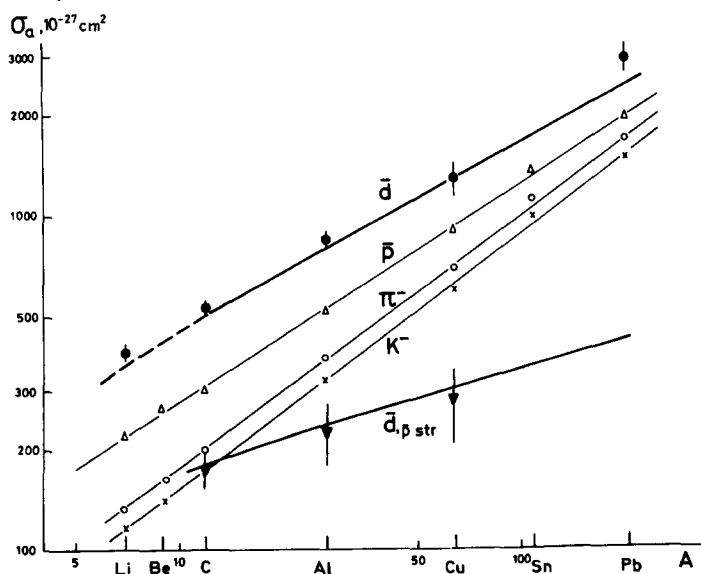


Fig. 4. Absorption cross sections of antideuterons (●), antiprotons (Δ), negative pions (○) and kaons (x) and the cross sections of antiproton stripping of antideuteron (▼) at  $P = 13.3$  GeV/c. The upper and the lower thick curves show the dependences of  $\sigma_{\bar{p}\text{str}}$  and  $\sigma_a$  upon the atomic weight  $A$  as calculated with the multiple scattering model [4]. Thin curves are power dependences  $\sigma_a \approx A^x$ , where  $x = 0.66$  ( $\bar{p}$ ),  $0.76$  ( $\pi^-$ ), and  $0.76$  ( $K^-$ ).

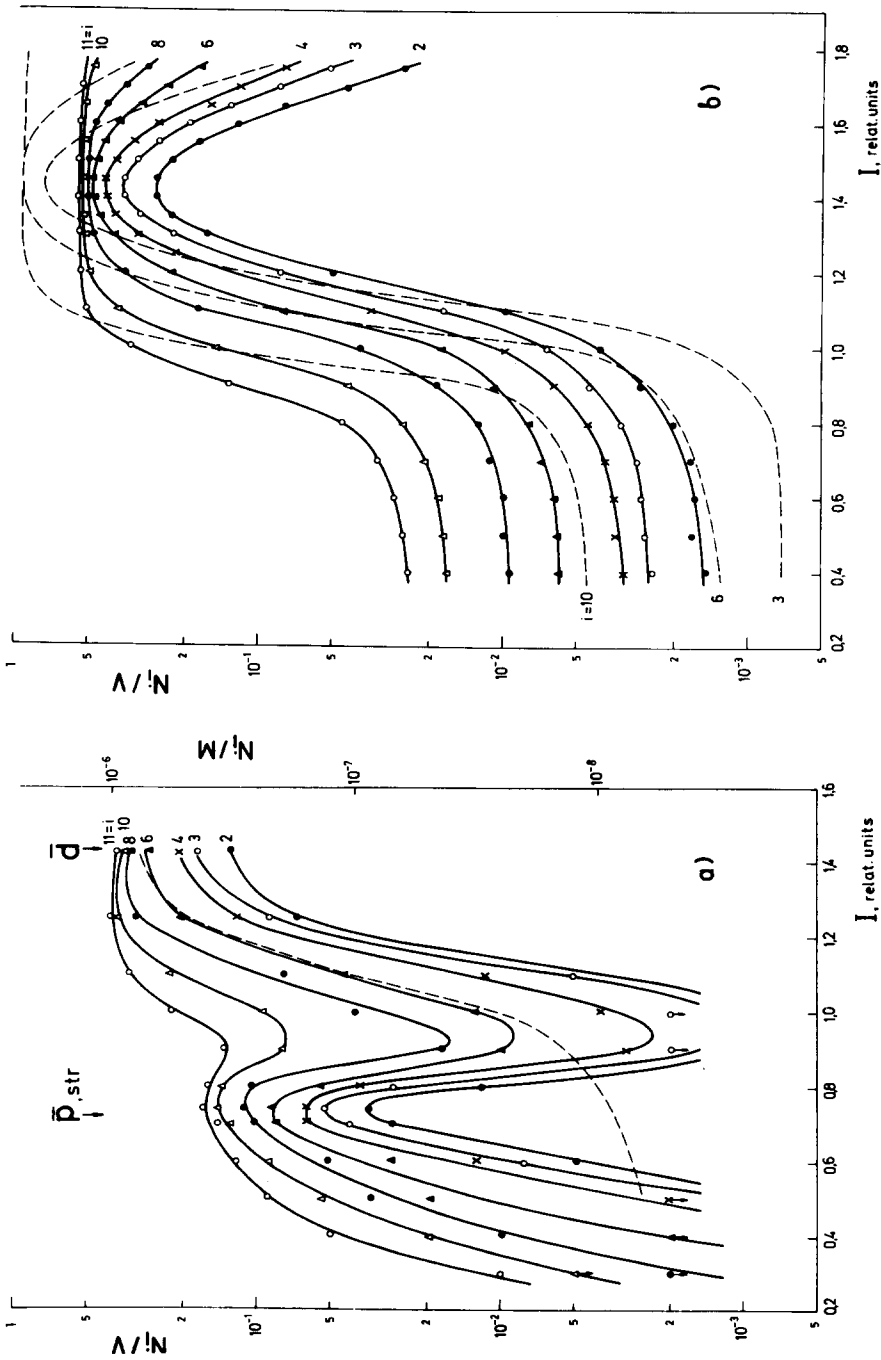


Fig. 5. The dependence of the counting rate of the transmission counters upon the current  $I$  of the magnet  $M_5$  measured in antideuteron (a) and in antiproton (b) beams. The curves are drawn by hand through the experimental points. The number of the counters  $i$  is indicated by the figures near the curves. Solid curves are the results of measurements with a carbon target in the beam; dashed curves (fig. b) are the same dependence measured with no target (only a part of data is presented in the figure in order not to overload it). A dashed curve (fig. a) is the background defined for  $i = 6$ .

#### 4. ANTIPROTON STRIPPING OF ANTIDEUTERONS

Antiprotons produced in the stripping of antideuterons in the target G have a momentum of 6.65 GeV/c, which is half the momentum of antideuterons, antiprotons and other particles in the beam striking the target. The magnet M<sub>5</sub> and the transmission counters T<sub>i</sub> were used as a magnetic spectrometer performing the momentum analysis of the particles and selected antiprotons produced in stripping. Fig. 5a presents the dependence of the counting rate  $N_i$  of the transmission counters on the current  $I$  of the magnet M<sub>5</sub> measured with a carbon target. At the current  $I \approx 0.7$ , i.e. at a half value of the beam momentum we observe a distinct peak in this dependence that corresponds to antiprotons in antideuteron stripping. A similar dependence measured in the antiproton beam on the same target shows monotonous behaviour (fig. 5b).

The counting rates of antiprotons from stripping  $n_i$  were defined via the peak values of the curves  $N_i(I)$  at  $I \approx 0.7$  (fig. 5a) after extracting the background from other particles produced in the target G. The background comprised less than 2% for  $i = 1 \div 3$  and increasing to 15% for  $i = 11$ . In determining the background the dependence  $N_i(I)$  (fig. 5b) was used. It was measured in the antiproton beam and normalized for the corresponding curves for antideuterons at  $I > 1.0$  (fig. 5a).

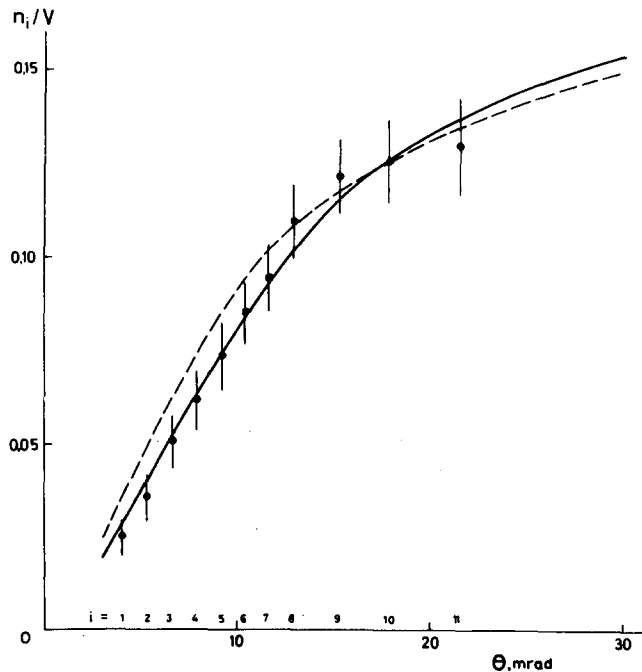


Fig. 6. Angular distribution of antiprotons from the stripping of antideuterons in carbon. Solid curves is the dependence  $\phi(\theta)$  calculated using the Salpeter-Goldstein distribution at  $\epsilon_d = 2.4$  MeV taking into account antiproton scattering in the target.

Dashed curve is the same, antiproton scattering is not considered.

The values obtained for  $n_i/V$  at the various angles  $\theta$  that corresponded to counters  $T_i$  are given in fig. 6. For the largest transmission counter  $T_{11}$ , the angle  $\theta$  was 21.5 mrad. If the momentum distribution of antinucleons in antideuteron is assumed to be similar to that of protons in deuterons (see below) then 85% of the total flux of antiprotons from the stripping of antideuterons are expected in the indicated angular range. A correction for antiproton absorption in the target (35% for carbon) was also taken into account when defining the cross section of antiproton stripping of antideuterons  $\sigma_{\bar{p}\text{str}}$ . The cross sections  $\sigma_{\bar{p}\text{str}}$  for Al and Cu were found in a similar way. Table 1 and fig. 4 present the values obtained.

In fig. 4 the measured antideuteron absorption and stripping cross sections are compared with the Glauber model [4]. In the calculations the total cross section of antinucleon-nucleon interactions was taken as 58 mbarn. As is obvious from fig. 4, the calculated curve gives a satisfactory description of the experimental data with respect to the dependence of antideuteron absorption cross sections on the atomic weight of the target nuclei. The cross sections for the antiproton stripping of antideuterons, calculated with the multiple scattering model are also in accord with the ones obtained in this experiment.

In the experiment performed previously with an antideuteron beam of  $P = 25 \text{ GeV}/c$ , it was assumed that the measured cross sections  $\sigma'_a$  did not contain the cross sections of antiproton stripping  $\sigma_{\bar{p}\text{str}}$ . However the analysis of the angular distribution of antiprotons produced in stripping (fig. 6) shows that a considerable part ( $\approx 50\%$ ) of the cross sections  $\sigma_{\bar{p}\text{str}}$  was included in the values  $\sigma'_a$  obtained in that paper. Consequently the corrections for antiproton stripping [3] that had been introduced there in defining the antideuteron absorption cross sections  $\sigma_a$  should be reduced. As can be seen from table 1, the absorption cross sections for antideuterons found at  $P = 25 \text{ GeV}/c$  than become close to the ones found in the present experiment.

## 5. BINDING ENERGY OF ANTIDEUTERON

The measured dependence  $n_i/V = \phi(\theta)$  (fig. 6) is an integral distribution of antiprotons from stripping over the emission angle  $\theta$  (or over the transverse momenta of antiprotons  $P_1 \approx 6.65 \theta \text{ GeV}/c$ ). In the range of angles  $\theta \gtrsim 8 \text{ mrad}$  the shape of the distribution is mainly defined by the momentum spectrum of antinucleons in antideuterons  $F(P_2)$ . At smaller angles, particle scattering in the target and the final size of the beam become important.

In the case of deuteron the momentum spectrum  $F(P_2)$  may be represented by the Salpeter-Goldstein distribution [11] that describes well the real spectrum  $F(P_2)$  up to the momenta  $P_2 \approx 300 \text{ MeV}/c$  [12]. At small  $P_2$  the distribution has the following form:

$$F(P_2) \approx P_2^2 (\gamma^2 + P_2^2)^{-2}, \quad (2)$$

where the parameter  $\gamma = 46 \text{ MeV}/c$  corresponds to the deuteron binding energy  $\epsilon_{\bar{d}} = 2.2 \text{ MeV}$ .

The angular dependence of stripping  $\phi(\theta)$  was calculated with the Salpeter-Goldstein distribution using the data on antiproton scattering in the target obtained in the beam with  $P = 6.65$  GeV/c (fig. 6). The value of the binding energy of antideuteron  $\epsilon_{\bar{d}}$  was obtained, using eq. (2), with the method of least squares by comparing the experimentally obtained angular distribution with the dependence  $\phi(\theta)$  calculated at different values of  $\epsilon_{\bar{d}}$ . The binding energy turned out to be

$$\epsilon_{\bar{d}} = 2.4 \pm 0.6 \text{ MeV}.$$

So, within the errors of measurements, the antideuteron binding energy coincides with that of deuteron, confirming the CPT invariance of nuclear forces.

In conclusion we would like to thank S. S. Gerstein and R. M. Suljaev for discussing the experimental results.

## REFERENCES

- [1] Yu. M. Antipov, N. K. Vishnevsky, Yu. P. Gorin, S. P. Denisov, S. V. Donskov, A. F. Yetch, A. M. Zaytzev, V. A. Kachanov, V. M. Kutjin, L. G. Landsberg, V. G. Lapshin, A. A. Lebedev, A. G. Morozov, A. I. Petrukhin, Yu. D. Prokoshkin, E. A. Razuvaev, V. I. Rykalin, V. I. Soljanic, D. A. Stojanova, V. P. Khromov and R. S. Shuvalov, IHEP preprint, 70-38, Serpukhov, 1970; Phys. Letters 34B (1971) 164
- [2] D. E. Dorfan, J. Eades, L. M. Lederman, W. Lee and S. C. C. Ting, Phys. Rev. Letters 14 (1965) 1003.
- [3] F. Binon, Yu. P. Gorin, S. P. Denisov, G. Giacomelli, S. V. Donskov, P. Duteil, V. A. Kachanov, V. M. Kutjin, J. P. Peigneux, A. I. Petrukhin, Yu. D. Prokoshkin, E. A. Razuvaev, D. A. Stojanova, J. P. Stroot and R. S. Shuvalov, IHEP preprint, 69-104, Serpukhov, 1969; Phys. Letters 31B (1970) 230.
- [4] G. Faltdt and H. Pilkuhn, CERN preprint TH 1064, 1969.
- [5] V. S. Barashenkov, K. K. Gudima and V. D. Toneev, Yad. Phys. 10 (1969) 760.
- [6] N. I. Golovnya, M. I. Grachev, K. I. Gubrienko, E. V. Eremenko, V. I. Kotov, V. S. Seleznev and Yu. S. Khodyrev, IHEP preprint, 70-28, Serpukhov, 1970.
- [7] S. V. Donskov, V. A. Kachanov, V. M. Kutjin, A. I. Petrukhin, Yu. D. Prokoshkin, E. A. Razuvaev and R. S. Shuvalov, IHEP preprint, 68-16-K, Serpukhov, 1968; PTE 3 (1969) 60.
- [8] Yu. M. Antipov, N. K. Vishnevsky, Yu. P. Gorin, S. P. Denisov, S. V. Donskov, F. A. Yetch, G. D. Zhilchenkova, A. M. Zaytzev, V. A. Kachanov, V. M. Kutjin, L. G. Landsberg, V. G. Lapshin, A. A. Lebedev, A. G. Morozov, A. I. Petrukhin, Yu. D. Prokoshkin, E. A. Razuvaev, V. I. Rykalin, V. I. Solyanic, D. A. Stojanova, V. P. Khromov and R. S. Shuvalov, IHEP preprint, 70-16, Serpukhov, 1970; Yad. Phys. 12 (1970) 311.
- [9] Yu. P. Gorin, S. P. Denisov, S. V. Donskov, A. F. Dunaitzev, A. I. Petrukhin, Yu. D. Prokoshkin, D. A. Stojanova and R. S. Shuvalov, IHEP preprint, 69-63, Serpukhov, 1969.
- [10] J. V. Allaby, Yu. B. Bushnin, Yu. P. Gorin, S. P. Denisov, G. Giacomelli, A. N. Diddens, R. W. Dobinson, S. V. Donskov, A. Klovning, A. I. Petrukhin, Yu. D. Prokoshkin, C. A. Stahlbrandt, D. A. Stojanova and R. S. Shuvalov, IHEP preprint, 69-87, Serpukhov, 1969; Yad. Phys. 12 (1970) 538.
- [11] E. Salpeter and G. Goldstein, Phys. Rev. 90 (1953) 983.
- [12] Yu. D. Prokoshkin, JETP (Sov. Phys.) 38 (1960) 455.